Available online at www.sciencedirect.com

ScienceDirect

Procedia Structural Integrity 5 (2017) 187–194

Structural Integrity Procedia

www.elsevier.com/locate/procedia

2nd International Conference on Structural Integrity, ICSI 2017, 4-7 September 2017, Funchal, Madeira, Portugal

Influence of the SMA Constitutive Model on the Response of Structures

Pedro Nunes[a], Paulo Silva Lobo[a,b,*]

[a]*Departamento de Engenharia Civil e Geologia, Universidade da Madeira, Campus Universitário da Penteada, 9000-390, Funchal, Portugal*
[b]*CERIS, Instituto Superior Técnico, Universidade de Lisboa, Av. Rovisco Pais 1, 1049-001, Lisboa, Portugal*

Abstract

Strong earthquakes may impose significant displacements in structures, which can result in excessive displacements at structural joints. Previous numerical studies have shown that the recentring capability of shape memory alloys (SMA) can be applied to limit joint openings and maximum longitudinal displacements. However, these studies do not focus on the influence of the SMA constitutive model adopted on the estimated displacements. A sensitivity analysis was performed using simplified two-degree-of-freedom models, which represent two-frame reinforced concrete bridges with various ratios of natural periods of vibration, connected by SMA bars. These models were implemented in a MATLAB based program for nonlinear dynamic analysis. The obtained results show that the relative displacements are more sensitive to the SMA model than the absolute displacements.

Peer-review under responsibility of the Scientific Committee of ICSI 2017

Keywords: Superelastic SMA; Uniaxial models; Kinetic law; Structural joint; Relative displacement.

1. Introduction

Superelasticity is a thermomechanical property of SMA which makes it possible for these metallic alloys to recover from large strains without significant residual strains. Although there are more than 30 known SMA, Nickel-Titanium (NiTi) alloys present the most interesting characteristics for seismic engineering applications: recovery from strains

* Corresponding author.
E-mail address: paulo.lobo@tecnico.ulisboa.pt

2452-3216
Peer-review under responsibility of the Scientific Committee of ICSI 2017
10.1016/j.prostr.2017.07.098

as high as 8%; fatigue resistance, of the order of hundreds 6%-8% axial strain cycles; operability on temperature ranging between -100 and 100 ºC; stable superelasticity, optimizable in the manufacturing process; durability due to high corrosion resistance and nondegradation of memory effects with martensite ageing (Otsuka and Ren, 1999; Dolce et al., 2000; Otsuka and Ren, 2004; Janke et al., 2005).

Superelastic NiTi may present two distinct crystalline structures, namely austenite (A) and the softer phase, detwinned martensite (M). In their undeformed state, superelastic NiTi are found in austenitic phase. When the material is subjected to applied loads, austenite transforms into detwinned martensite, in a solid-solid reversible transformation process called direct transformation. In the unloading phase, the detwinned martensite transforms into austenite, the so-called reverse transformation, in which the original form is recovered. Depending on the type of alloy, different tension and compression behaviour may be observed (Lim and McDowell, 1999). Stabilization of the NiTi alloy superelasticity may be obtained through cyclic training (Dolce and Cardone, 2001). Trained NiTi alloys maintain the recentring capacity for many complete and incomplete cycles, without significant residual strains, independent of strain rate, maximum strain, ambient temperature and SMA geometry (Dolce and Cardone, 2001; McCormick et al., 2007). This makes NiTi suitable for application in recentring devices.

The superelastic behaviour is dependent on the SMA temperature, a function of the ambient temperature and of the strain rate. With the increase of the latter parameter, latent heat originating at the transformation phases may result in significant temperature variations, changing the critical stresses at which phase transformation starts (s) and finishes (f), namely σ_s^{AM}, σ_f^{AM}, σ_s^{MA} and σ_f^{MA}, according to the Clausius-Clapeyron law, which affects the hysteretic response and, consequently, the energy dissipated by the SMA. For the range of frequencies of vibration of interest for earthquake engineering applications (0.1-5 Hz), energy dissipation capacity of NiTi alloys, in terms of equivalent viscous damping, ζ_{eq}, ranges from 5% to 10%, and tends to increase with the decrease of the SMA diameter (DesRoches et al. 2004; McCormick et al. 2006). It should be noted that these are low values for civil engineering applications, thus the recentring capacity is the key point on passive applications of SMA.

Several constitutive models intended to predict the superelastic response of SMA have been proposed. A review on this material may be found in Silva Lobo et al. (2015). Andrawes and DesRoches (2005, 2007a, 2007b, 2007c) and Johnson et al. (2008) applied SMA constitutive models to evaluate the effectiveness of superelastic SMA on the control of displacements of multi-frame reinforced concrete (RC) bridges, with various natural period ratios, submitted to earthquakes. Both authors adopted a two-degree-of-freedom oscillator (TDOF), consisting of two frames coupled by SMA bars or wires. However, none of these studies compared the influence of different constitutive models in the values of relative and absolute displacements. Du et al. (2005) and Andrawes and DesRoches (2008) are the exceptions, but they focused only the absolute displacements. The former study was performed using a single-degree-of-freedom oscillator (SDOF) fixed to the exterior by a SMA element. A nonlinear temperature dependent model, coupled with the cosine kinetic law presented by Liang and Rogers (1990), and a linear and temperature independent model were used to simulate the SMA. These authors reported minor influence of the SMA constitutive model on the response of the considered structure. The latter study also adopted a SDOF model fixed by a SMA element. A linear and temperature independent model, a nonlinear and temperature dependent model, and a model similar to the latter with the added capability of accounting for the unstable superelasticity of untrained superelastic SMA were used. The last two models were coupled with the Tanaka et al. (1986) kinetic law. An isothermal dynamic analysis was performed, resulting in differences of 9% to 39% with the different SMA models.

In this study, three SMA constitutive models were adopted. These models were used to describe the axial behaviour of superelastic SMA bars in nonisothermal conditions connecting the two frames of two-frame RC bridges. The objective is to evaluate the influence of SMA model on both absolute and relative displacements.

2. Uniaxial constitutive models for superelastic SMA

Although tridimensional models have been proposed, uniaxial macroscale models are adequate to characterize the axial behaviour of SMA in their most usual form, namely bars and wires. In the research presented herein a family of uniaxial macroscale models based on the work by Tanaka et al. (1986) was adopted. These models are dependent on temperature and strain rate, thus they may be applied for both quasi-static and dynamic loading. The coupling of three laws is considered, namely the mechanical, the kinetic and the heat balance laws. More detail on these models may be found in other documents (Silva Lobo et al., 2015).

The mechanical law relates stress, strain and martensitic fraction, ξ. Identical results were obtained with models based on the schemes of Voigt, Reuss and Mori-Tanaka (Auricchio and Sacco, 1997) when the same kinetic law was used (Brinson and Huang, 1996). For the purpose of this study, the Voigt model was adopted, thus it results

$$\sigma = E(\xi)\text{x}\,(\varepsilon - \varepsilon_L \text{ x } \xi) + \Theta(T - T_0) \quad \text{with} \quad E(\xi) = E_A + (E_M - E_A) \text{ x } \xi \tag{1}$$

where σ is the axial stress, ε is the axial strain, ε_L is the maximum residual strain, Θ is the modulus of thermoelasticity, T is the SMA temperature and T_0 is the ambient temperature. E_A and E_M are the pure austenite and martensite Young's modulus, respectively.

The kinetic law governs the changes in the SMA crystalline structure, as a function of σ and T. The most relevant kinetic laws seem to be the cosine law (Liang and Rogers, 1990; Brinson, 1993), the exponential laws (Tanaka et al., 1986; Lubliner and Auricchio, 1996), and the linear law (Auricchio and Sacco, 1997). These laws are expressed by ξ^{AM}, for the direct transformation, and by ξ^{MA}, for the reverse transformation.

The cosine law is given by

$$\xi^{AM} = \frac{1-\xi_0}{2} \text{ x } \cos\left[\frac{\pi}{M_s - M_f}\left(T - M_f - \frac{\sigma}{\text{C}_\text{M}}\right)\right] + \frac{1+\xi_0}{2} \quad \text{and} \quad \xi^{MA} = \frac{\xi_0}{2}\, x \left\{cos\left[\frac{\pi}{A_f - A_s}\left(T - A_s - \frac{\sigma}{C_A}\right)\right] + 1\right\} \tag{2}$$

where ξ_0 is the fraction of martensite observed in the previous phase transformation, M_s, M_f, A_s and A_f are the transition temperatures for direct and reverse transformations in the stress-free state. C_M and C_A are the Clausius-Clapeyron coefficients, which take into account the linear increase of the SMA critical stresses as a function of T (Brinson, 1993). Because the phase transformations depend on the value of ξ_0 (Brinson and Huang, 1996), this parameter must be included in all kinetic laws, making it possible to consider the effect of incomplete transformation cycles. With this in mind, the exponential kinetic law adopted by Tanaka et al. (1986) (Exponential_T) may be rewritten as (Silva Lobo et al., 2015)

$$\xi^{AM} = (\xi_0 - 1) \text{ x } e^{[a_M(M_s - T) + b_M\sigma]} + 1 \quad \text{and} \quad \xi^{MA} = \xi_0 \text{ x } e^{[a_A(A_s - T) + b_A\sigma]} \tag{3}$$

where $a_M = -2\,ln(10)\,/(M_s - M_f)$, $b_M = a_M(M_s - M_f)/(\Delta\sigma_M)$, $a_A = 2ln(10)/(A_f - A_s)$ and $b_A = a_A(A_f - A_s)/(\Delta\sigma_A)$, in which $\Delta\sigma_M$ and $\Delta\sigma_A$ are the width along the stress axis of the martensitic and austenitic transformation strips.

Alternatively, Lubliner and Auricchio (1996) adopted the exponential kinetic law given by

$$\xi^{AM} = (1-\xi_0) \text{ x } \left[1 - e^{\left[-\beta_M \text{ x } \left(\frac{1}{\text{C}_\text{M}(T - M_f) - \sigma} - \frac{1}{\text{C}_\text{M}(M_s - M_f)}\right)\right]}\right] + \xi_0 \quad \text{and} \quad \xi^{MA} = \xi_0\, x \left[e^{\left[-\beta_A \text{ x } \left(\frac{1}{\sigma - \text{C}_\text{A}(T - A_f)} - \frac{1}{\text{C}_\text{A}(A_f - A_s)}\right)\right]}\right] \tag{4}$$

where β_M and β_A are parameters that adjust the slope of the transformation phases. Lubliner and Auricchio (1996) adopted $\beta_M = \beta_A = 3$ MPa.

Including the ξ_0 modification, linear kinetic law (Linear) may be rewritten as

$$\xi^{AM} = (1-\xi_0) \text{ x } \frac{|\sigma| - \sigma_s^{AM}}{\sigma_f^{AM} - \sigma_s^{AM}} + \xi_0 \quad \text{and} \quad \xi^{MA} = \xi_0 \text{ x } \frac{|\sigma| - \sigma_f^{MA}}{\sigma_s^{MA} - \sigma_f^{MA}} \tag{5}$$

The heat balance law, presented in the Equation in (6), makes it possible to estimate the value of T of bars and wires of SMA as a function of the strain time-history. This law may be integrated using the backward Euler method (Vitiello et al., 2005).

$$\frac{dT(t)}{dt} = \frac{\left(c_L \text{ x } \rho \text{ x } \frac{d\xi}{dt}\right) \text{ x } V - h \text{ x } A_i \text{ x } (T(t) - T_0)}{\rho \text{ x } c_p \text{ x } V} \tag{6}$$

c_L is the latent heat, V is the specimen volume, h is the convection heat transfer coefficient, A_i is the interface area, ρ is the density of the material and c_p is the specific heat. $d\xi / dt$ may be estimated with finite difference approximations.

Fig. 1 shows a generic isothermal stress-strain curve for each kinetic law presented above. For the exponential law adopted by Lubliner and Auricchio (1996), the same values for β_M and β_A adopted by these authors were used (Exponential_LA3). For the analysis described below, $\beta_M = \beta_A = 20$ MPa (Exponential_LA20) were also used, for generality of the performed assessment, in which case this kinetic law becomes closer to the linear alternative. The cosine kinetic law was not used, because, as can be seen in Fig. 1, it results similar to the linear kinetic law.

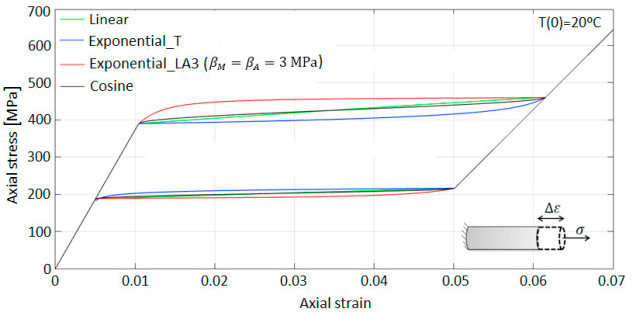

Fig. 1. General stress-strain curves for all the kinetic laws considered.

3. Assessment of a RC bridge with SMA

To evaluate the influence of the SMA constitutive model on the response of structures, a two-span RC bridge (see Fig. 2) was selected from Mehr and Zaghi (2016). The specified materials are A400 NR for steel and C35/45 for concrete. The properties of the SMA used by Cismaşiu and Santos (2008) were adopted. Frames 1 and 2 have $m_1 = 3617.7$ ton and $m_2 = 4304.2$ ton, respectively. Both frames are supported by three RC columns with diameter $D = 2$ m, with 50 ϕ40 longitudinal rebars and ϕ20 hoops spaced at 0.11 m. The cracked flexural stiffness of the columns cross-section was estimated according to Priestley et al. (2007). The height of the columns of the frame 2, H_2, was fixed to obtain a natural period of vibration, T_2, of 1.0 s, and the values of H_1 were calculated to obtain different natural periods of vibration, T_1.

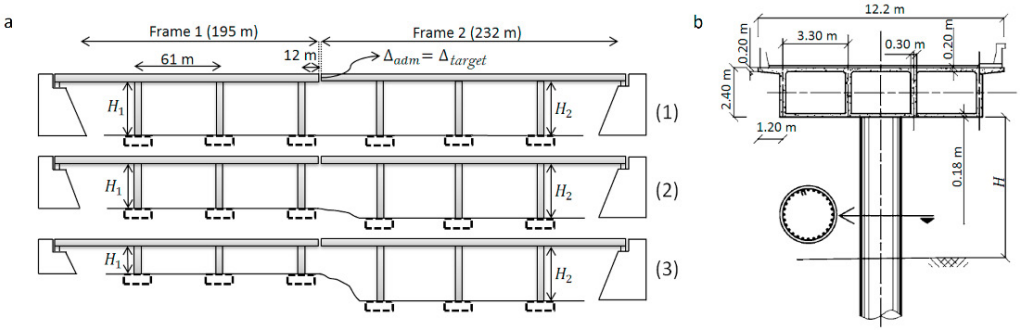

Fig. 2. (a) longitudinal profile; (b) transverse profile.

Together with the Newmark β-method, with $\gamma = 1/2$ e $\beta = 1/4$, the linear TDOF model presented in Fig. 3 was considered, making it possible to simulate, in a simplified manner, the longitudinal dynamic response of the bridge submitted to a given accelerogram. A viscoelastic damping ratio of 5% was used and the two frames were considered coupled by a superelastic SMA.

Six seismic records were selected to perform a sensitivity analysis. Their characteristics, namely magnitude, shortest distance from the structure to the epicenter (Rrup), peak ground acceleration (PGA) and duration, are presented in Table 1.

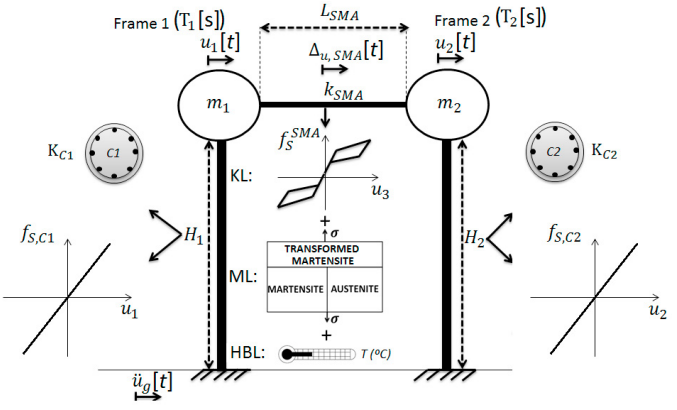

Fig. 3. TDOF used in the sensitivity analysis.

Table 1. Characteristics of the seismic records used in the sensitivity analysis.

Seismic record	Moment magnitude scale	R_{rup} [km]	PGA [%g]	Duration [s]
Loma Prieta (Corralitos)	6.93	3.85	0.645	13.95
Loma Prieta (Gilroy Array #3)	6.93	12.82	0.559	9.98
Kobe (Nishi-Akashi)	6.90	7.09	0.480	16.65
São Fernando (Pacolma Dam)	6.61	1.81	0.687	10.72
Northridge (Canonga Park)	6.69	14.70	0.358	17.92
Umbria and Merche (Colfiorito)	6.00	6.92	0.198	8.89

First of all, the TDOF was simulated for all ratios of natural periods of vibration, T_1/T_2, and for all six seismic records. The results of these analyses are shown in Fig. 4 (a). As can be seen, the Corralitos seismic record causes, in general, the higher values of absolute relative hinge displacement (ARHD). Thus, this seismic record, as well as the linear kinetic law and $T_0 = 20$ ºC, were considered as references for the SMA design. This was performed by determination of the values of the cross-section area of the SMA, A_{SMA}, which make it possible to attain ARHD equal to the objective displacements, $\Delta_{u,target}$, chosen to be equal to ARHD/3. Given the characteristics of the SMA, a strain limit of 6% was adopted. The maximum value of ARHD is 0.194 m, thus it results $\Delta_{u,target} = 0.064$ m and, accordingly, a SMA length given by $L_{SMA} = 0.0638/0.06 = 1.063$ m. Because values of $T_1/T_2 < 0.5$ are not expected in a real bridge design, and for $T_1/T_2 \geq 0.9$ the required values of A_{SMA} are very low, because the vibration of the structures are close to be in phase, values from 0.5 to 0.8 s, in steps of 0.1 s, were considered in this study. The determined values of A_{SMA} are shown in Fig. 4 (b).

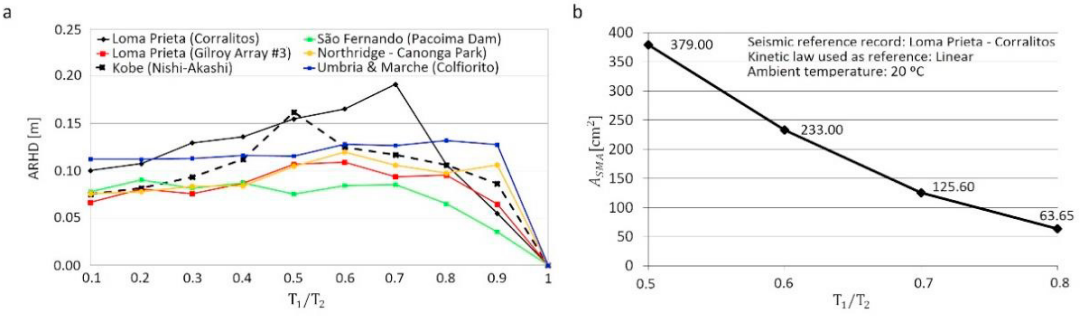

Fig. 4. (a) dynamic analysis of the structure without SMA; (b) cross-section area of the SMA.

The results of the two frames coupled by the SMA for the Corralitos seismic record are presented below. The absolute displacements of each frame, with and without the SMA element, are presented in Fig. 5 (a). As can be seen, the introduction of the SMA made it possible to reduce the values of $u_{1,abs}$ for all cases, while $u_{2,abs}$ increase. In Fig. 5 (b), a comparison between these displacements and those of the nonlinear kinetic laws (|[[u(Linear)- u(nonlinear kinetics)]/ u (Linear)]|x100) is presented. The maximum u relative difference value is 16%. However, for the remaining analyses, u relative differences are less than 10% and tend to decrease with the increase of T_1/T_2. In Fig. 5 (c), the relative displacements obtained with all kinetic laws, as well as without the SMA, for comparison, are shown. Finally, in Fig. 5 (d), the differences on the ARHD are presented. Even though the relative differences are, in general, lower than 15%, a 32% difference was obtained. This seems to indicate that relative displacements are more sensitive to the adopted kinetic law than absolute displacements.

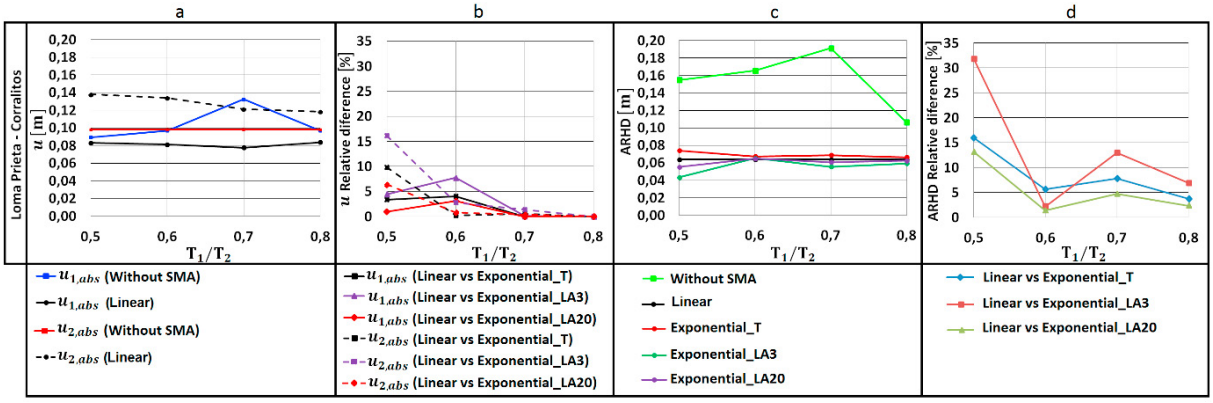

Fig. 5. Results of the sensitivity analysis for the Corralitos seismic record.

The results for the other seismic records considered are presented in Fig. 6. This figure shows that it is not possible to define a trend for the response of the considered structure. This is because the SMA were not designed for the seismic records considered in each analysis. Coherently with the reason that motivated the choice of the Corralitos seismic record as reference for design of the SMA elements, presented above, it can be seen that the ARHD values are lower than the target displacements.

Observing Fig. 5 and 6, it can be seen that, although the introduction of the SMA element makes it possible to better control $u_{1,abs}$, this is not without exception, depending on the characteristics of the earthquake considered. Furthermore, the relative differences in absolute displacements are less than 10%. Regarding AHRD, the relative differences are significantly higher. The obtained results indicate that, in the case of the absolute displacements, the choice of the kinetic law is not as relevant as for the determination of the AHRD, in which case the maximum relative difference is of 31%. These differences are due to the different hysteretic characteristics of the kinetic laws, which result in different values of energy dissipation. As could be expected, in general, the most effective law to control the AHRD of the assessed structure is the one which makes it possible to dissipate more energy (Exponential_LA3).

The values of the strain experienced by the SMA does not present a correlation with the AHRD relative differences, because high values are observed for both high and low-strain values of the SMA. For small values of strain, there are two particularities which should be noted: when the SMA remains elastic, which occurred, for example, for the Umbria and Marche seismic record for $T_1/T_2 = 0.5$ and for $T_1/T_2 = 0.6$, the AHRD relative difference is null (for these cases, u relative differences are also close to null); when the SMA experiences little nonlinear behaviour, which occurred for the same seismic record, for $T_1/T_2 = 0.7$, and for the Pacoima Dam accelerogram, the energy dissipated is small and the AHRD relative differences also result small. For these cases, u relative differences are small or null. For the other cases, a clear correlation between AHRD and the absolute displacements has not been identified.

It should be noted that intense earthquakes may result in residual displacements of RC or steel structures. This was not focused on this paper, but the influence of the SMA constitutive models on the prediction of residual displacements using numerical analysis should also be assessed in the future.

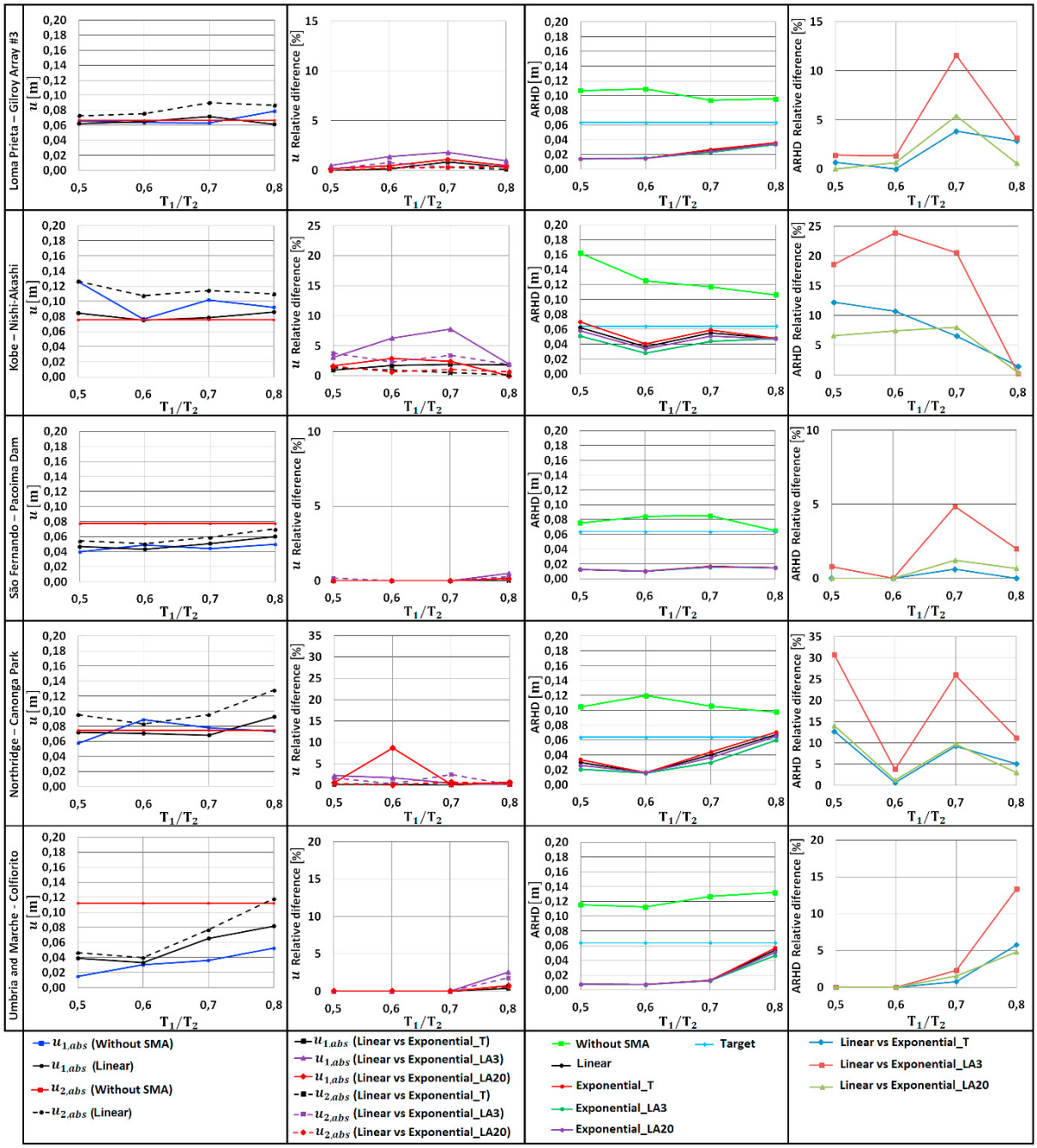

Fig. 6. Results of the sensitivity analysis for five seismic records.

4. Conclusions

This paper focus on the numerical assessment of the response of structures with SMA modelled by a family of uniaxial macroscale models based on the work by Tanaka et al. (1986). A sensitivity study was conducted using a linear TDOF, which represents two-frame RC bridges, to evaluate the influence of different kinetic laws on the structural response. The model was implemented in a MATLAB based program for nonlinear dynamic analysis of

structures using the Newmark β-method. For the 24 analyses performed, the maximum relative difference of the absolute displacement of the frames of the structures considered is 16%. On the other hand, the maximum relative difference of the AHRD is 32%. Thus, the obtained results indicate that this parameter may be highly sensitive to the constitutive model of the SMA. As such, the choice of the kinetic law may be relevant for the seismic design of structures with SMA elements. The obtained differences could, depending on the adopted safety factors, compromise the structural integrity, thus the SMA constitutive model should be carefully calibrated using experimental data.

References

Andrawes, B., DesRoches, R., 2005. Unseating Prevention for Multiple Frame Bridges Using Superelastic Devices. Smart Materials and Structures 14(3), S60–S67.

Andrawes, B., DesRoches, R., 2007a. Comparison Between Shape Memory Alloy Seismic Restrainers and Other Bridge Retrofit Devices. Journal of Bridge Engineering 12 (6), 700–709.

Andrawes, B., DesRoches, R., 2007b. Effect of Hysteretic Properties of Superelastic Shape Memory Alloys on the Seismic Performance of Structures. Structural Control and Health Monitoring 14(2), 301–320.

Andrawes, B., DesRoches, R., 2007c. Effect of Ambient Temperature on the Hinge Opening in Bridges with Shape Memory Alloy Seismic Restrainers. Engineering Structures 29(9), 2294–2301.

Andrawes, B., DesRoches, R., 2008. Sensitivity of Seismic Applications to Different Shape Memory Alloy Models. Journal of Engineering Mechanics 134(2), 173–183.

Auricchio, F., Sacco, E., 1997. A One-Dimensional Model for Superelastic Shape-Memory Alloys with Different Elastic Properties Between Austenite and Martensite. International Journal of Non-Linear Mechanics 32(6), 1101–1114.

Brinson, L. C., 1993. One-Dimensional Constitutive Behavior of Shape Memory Alloys: Thermomechanical Derivation with Non-Constant Material Functions and Redefined Martensite Internal Variable. Journal of Intelligent Material Systems and Structures 4(2), 229–242.

Brinson, L. C., Huang, M. S., 1996. Simplifications and Comparisons of Shape Memory Alloy Constitutive Models. Journal of Intelligent Material Systems and Structures 7(1), 108–114.

Cismaşiu, C., Santos, F., 2008. Numerical Simulation of Superelastic Shape Memory Alloys Subjected to Dynamic Loads. Smart Materials and Structures 17(2), 25–36.

DesRoches, R., McCormick, J., Delemont, M., 2004. Cyclic Properties of Superelastic Shape Memory Alloy Wires and Bars. Journal of Structural Engineering 130(1), 38–46.

Dolce, M., Cardone, D., Marnetto, R., 2000. Implementation and Testing of Passive Control Devices Based on Shape Memory Alloys. Earthquake Engineering and Structural Dynamics 29(7), 945–968.

Dolce, M., Cardone, D., 2001. Mechanical Behaviour of Shape Memory Alloys for Seismic Applications: Austenite NiTi Wires Subjected to Tension. International Journal of Mechanical Sciences 43(11), 2657–2677.

Du, X., Sun, G., Sun, S., 2005. Piecewise Linear Constitutive Relation for Pseudo-Elasticity of Shape Memory Alloy (SMA). Materials Science and Engineering: A 393(12), 332–337.

Janke, L., Czaderski, C., Motavalli, M., Ruth, J., 2005. Applications of Shape Memory Alloys in Civil Engineering Structures - Overview, Limits and New Ideas. Materials and Structures 38(279), 578–592.

Johnson, R., Padgett, J. E., Maragakis, M. E., DesRoches, R., Saiidi, M.S., 2008. Large Scale Testing of Nitinol Shape Memory Alloy Devices for Retrofitting of Bridges. Smart Materials and Structures 17(3), pp. 10.

Liang, C., Rogers, C. A., 1990. One-Dimensional Thermomechanical Constitutive Relations for Shape Memory Materials. Journal of Intelligent Material Systems and Structures 1(2), 207–234.

Lim, T., McDowell, D., 1999. Mechanical Behavior of an Ni-Ti Alloy Under Axial-Torsional Proportional and Non-Proportional Loading. Journal of Engineering Materials and Technology 121(1), 9–18.

Lubliner, J., Auricchio, F., 1996. Generalized Plasticity and Shape-Memory Alloys. International Journal of Solids and Structures 33(7), 991–1003.

McCormick, J., DesRoches, R., Fugazza, D., Auricchio, F., 2006. Seismic Vibration Control Using Superelastic Shape Memory Alloys. Journal of Engineering Materials and Technology 128(3), 294–301.

McCormick, J., Tyber, J., DesRoches, R., Gall, K., Maier, H. J., 2007. Structural Engineering with NiTi. II: Mechanical Behavior and Scaling. Journal of Engineering Mechanics 133(9), 1019–1029.

Mehr, M., Zaghi, A. E., 2016. Seismic Response of Multi-Frame Bridges. Bulletin of Earthquake Engineering 14(4), 1219–1243.

Otsuka, K., Ren, X., 1999. Recent Developments in the Research of Shape Memory Alloys. Intermetallics 7(5), 511–528.

Otsuka, K., Ren, X., 2004. Mechanism of Martensite Aging Effect. Scripta Materialia 50(2), 207–212.

Priestley, M. J. N., Calvi, G. M., Kowalsky, M. J., 2007. Displacement-Based Seismic Design of Structures. IUSS Press, Pavia, Italy, pp. 721.

Silva Lobo, P., Almeida, J., Guerreiro, L., 2015. Shape Memory Alloys Behaviour: A Review. Procedia Engineering 114, 776–783.

Tanaka, K., Kobayashi, S., Sato, Y., 1986. Thermomechanics of Transformation Pseudoelasticity and Shape Memory Effect in Alloys. International Journal of Plasticity 2(1), 59–72.

Vitiello, A., Giorleo, G., Morace, R. E., 2005. Analysis of Thermomechanical Behaviour of Nitinol Wires with High Strain Rates. Smart Materials and Structures 14(1), 215–221.